Phase Equilibria at liquidus temperatures of the $CaO{\cdot}SiO_2$–$Na_2O{\cdot}SiO_2$—$Na_2O{\cdot}Al_2O_3{\cdot}6SiO_2$ Slag System

Zhan ZHANG[1)], Yanping XIAO[1)2)], Jack VONCKEN[3)], Yongxiang YANG[1),4)], Rob BOOM[1)], Nan WANG[4)] and Zongshu ZOU[4)]*

1) Department of Materials Science and Engineering, Delft University of Technology, 2628 CD, Delft, The Netherlands

2) Department of Metallurgical Engineering, Anhui University of Technology, 243002, Ma'anshan, China

3) Department of Geotechnology, Delft University of Technology, 2628 CN, Delft, The Netherlands

4) Department of Ferrous Metallurgy, Northeastern University, 110819, Shenyang, China

Abstract: Direct utilization and land filling of the bottom ash from municipal solid waste incineration (MSWI) can cause leaching of heavy metals and weathering problems. Vitrification is an efficient treatment technology which can transform the ash into stabilized glassy slag. Total amount of CaO, SiO_2, Al_2O_3, Fe_2O_3, Na_2O and MgO accounts for more than 90 wt% of the vitrified bottom ash slag for most of the Dutch MSWI bottom ashes. In order to better use the vitrified slag, the knowledge of the thermodynamic properties and phase relations of the related slag system is required. In the present work, the phase relations of a part of the CaO—SiO_2—Al_2O_3—Na_2O system were investigated. The region of the tetrahedron $CaO{\cdot}SiO_2$—$Na_2O{\cdot}SiO_2$—$Al_2O_3{\cdot}SiO_2$—SiO_2 which includes the bottom ash slag composition is on the focus in this research. Within this tetrahedron, the phase equilibria of the system $CaO{\cdot}SiO_2$—$Na_2O{\cdot}SiO_2$—$Na_2O{\cdot}Al_2O_3{\cdot}6SiO_2$ was experimentally studied at temperatures from 800 °C to 1200 °C.

The liquidus temperature was determined with differential scanning calorimetry (DSC). The equilibrium experiments at liquidus temperatures were conducted under argon gas. The equilibrated samples were quenched with pressurized nitrogen, and examined with electron probe micro analysis (EPMA) and X-ray diffraction (XRD) for identification of microstructure and phase relations. Five primary phase fields, $CaO{\cdot}SiO_2$, $Na_2O{\cdot}SiO_2$, $Na_2O{\cdot}2CaO{\cdot}3SiO_2$, $2Na_2O{\cdot}CaO{\cdot}3SiO_2$ and $Na_2O{\cdot}Al_2O_3{\cdot}6SiO_2$ were established. Three ternary invariant points were determined. Based on these experimental results, the projection of liquidus surface has been constructed from 800 °C to 1200 °C for the region focused in the present work.

Key words: Municipal solid waste incineration (MSWI), Bottom ash, Vitrification, Slag, Liquidus temperature, Phase relations.

1. Introduction

Waste-to-Energy combustion or incineration is an effective technology to convert municipal solid waste (MSW) to energy and can reduce the volume of wastes by approximately 90% [1]. On the other hand, this process produces a large amount of solid residues (approximately 25% of the MSW input) in which bottom ash accounts for about 85% by weight [2]. Leaching of heavy metals is a potential problem for recycling and utilization of the bottom ash. Vitrification is an efficient treatment technology of the bottom ash which can completely destroy the toxic organics, immobilize the heavy metals and reduce significantly the volume of the solid residues. Previous study indicated that the primary oxide

components of the vitrified bottom ash slag from a Dutch MSW incinerator are CaO, SiO_2, Al_2O_3, Na_2O, Fe_2O_3 and MgO [3]. In total they account for more than 90% of the slag by weight. These compositions have direct effect on the glass formation during vitrification, and further on the mineralogical and mechanical properties of the slag. Several studies [4, 5, 6] have been reported for the use of bottom ash in glass-ceramic products. In order to provide essential fundamental knowledge for recycling and utilization of the bottom ash, the multi-oxide system $CaO–SiO_2–Al_2O_3–Na_2O–Fe_2O_3–MgO$ should be investigated systematically.

The four oxides CaO, SiO_2, Al_2O_3 and Na_2O account for approximately 85% by weight of the above mentioned six oxides system. Therefore, the quaternary oxide system $CaO─Al_2O_3─SiO_2─Na_2O$ was mainly investigated in the present work. The normalized compositions of the vitrified bottom ash with these four oxides are 19.1 wt% CaO, 14.4 wt% Al_2O_3, 61.5 wt% SiO_2 and 5.0 wt% Na_2O. The position of the bottom ash composition in the $CaO─Al_2O_3─SiO_2─Na_2O$ tetrahedron is shown as the point P in Figure 1.

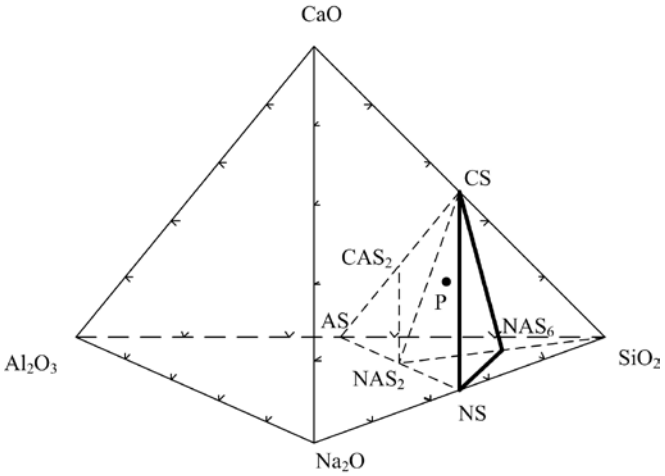

Fig. 1 The $CaO─Al_2O_3─SiO_2─Na_2O$ tetrahedron (A=Al_2O_3; C=CaO; N=Na_2O; S=SiO_2). P=Position of the bottom ash slag in the quaternary system.

Morey and Bowen [7] studied the phase relations of pseudo-binary system $CaO·SiO_2─Na_2O·SiO_2$ which is very important as a glass-ceramic system. Morey [8] investigated the phase equilibria in the more than 50 wt% silica region of $CaO·SiO_2─Na_2O·SiO_2$ in greater detail. The ternary eutectic point at which quartz coexists with $Na_2O·3CaO·6SiO_2$ and $Na_2O·2SiO_2$ was established at 725 °C. For the ternary system $Na_2O─CaO─SiO_2$ at less than 50 wt% SiO_2, equilibrium phase relations were experimentally investigated at temperatures between 1200 °C to 1400 °C in a previous study [9]. Six primary phase fields, $2CaO·SiO_2$, $3CaO·2SiO_2$, $CaO·SiO_2$, $Na_2O·2CaO·3SiO_2$, $Na_2O·2CaO·2SiO_2$ and $Na_2O·CaO·SiO_2$ were identified, and three invariant points were determined.

Furthermore, investigations were carried out on portions of the four-component system $CaO─Al_2O_3─SiO_2─Na_2O$ [10, 11, 12]. $Na_2O·Al_2O_3·6SiO_2$, $Na_2O·Al_2O_3·2SiO_2$, $CaO·Al_2O_3·2SiO_2$, $CaO·SiO_2$, $Na_2O·SiO_2$ and $Al_2O_3·SiO_2$ are the primary compounds in high SiO_2-containing region. The liquidus surface in the $CaO·SiO_2─Na_2O·SiO_2─Na_2O·Al_2O_3·2SiO_2$ subsystem was investigated by Spivak [10]. Three binary subsystems $CaO·SiO_2─Na_2O·SiO_2$, $Na_2O·SiO_2─Na_2O·Al_2O_3·2SiO_2$ and $CaO·SiO_2─Na_2O·Al_2O_3·2SiO_2$ were studied firstly. The phase relations in this ternary system were determined and three ternary invariant points were established with a

quenching method. Phase equilibria in the system $CaO{\cdot}SiO_2$─$CaO{\cdot}Al_2O_3{\cdot}2SiO_2$─$Na_2O{\cdot}Al_2O_3{\cdot}2SiO_2$ were investigated experimentally by Gummer [11]. The thermodynamic properties of the compound $Ca_2Al_2SiO_7$ were also studied. Foster [12] investigated the high temperature equilibrium relationships of the systems $CaO{\cdot}SiO_2$─$Na_2O{\cdot}Al_2O_3{\cdot}2SiO_2$, $CaO{\cdot}SiO_2$─$Na_2O{\cdot}Al_2O_3{\cdot}6SiO_2$ and $CaO{\cdot}SiO_2$─$Na_2O{\cdot}Al_2O_3{\cdot}2SiO_2$─$Na_2O{\cdot}Al_2O_3{\cdot}6SiO_2$. In the system $CaO{\cdot}SiO_2$─$Na_2O{\cdot}Al_2O_3{\cdot}6SiO_2$, the phase structure of $Na_2O{\cdot}Al_2O_3{\cdot}6SiO_2$ was reported, and it is not pure albite but rather a plagioclase bearing a small amount of anorthite. The liquidus temperatures between $CaO{\cdot}SiO_2$ and $Na_2O{\cdot}Al_2O_3{\cdot}6SiO_2$ (pseudo-binary system) were determined. The eutectic composition and temperature was established at ~87 wt% $CaO{\cdot}SiO_2$ and ~1140 °C, respectively. Phase equilibria in the glass-forming region of the system CaO─Al_2O_3─SiO_2─Na_2O were studied by Moir and Glasser [13]. The liquidus diagram of the Al_2O_3-SiO_2-Na_2O system and isothermal section at 770°C of the CaO- SiO_2-Na_2O were presented. The quaternary system was studied by taking isoplethal sections at 5.0 wt%, 10.0 wt% and 15.0 wt% Al_2O_3. The temperatures and approximate compositions of the quaternary liquidus invariant points were given under the subsolidus equilibria conditions.

Reviewing the literature information on the $CaSiO_3$-Na_2SiO_3 pseudo-binary system and the $CaO{\cdot}SiO_2$─$Na_2O{\cdot}SiO_2$─$Al_2O_3{\cdot}SiO_2$─SiO_2 pseudo-quaternary system, the phase relations of the pseudo-ternary system $CaO{\cdot}SiO_2$─$Na_2O{\cdot}SiO_2$─$Na_2O{\cdot}Al_2O_3{\cdot}6SiO_2$, which are important for bottom ash applications, however, were scarcely reported. In the present work this pseudo-ternary system was experimentally investigated under controlled high-temperature equilibrium conditions.

2. Experimental

2.1 Sample preparation

Laboratory reagent grade powders of CaO (99.5 wt%), SiO_2 (99.7 wt%), Na_2CO_3 (99.5 wt%) and Al_2O_3 (99.7 wt%) were used as starting materials. Heat treatment before equilibrium experiments – dehydration ensured the anhydrous condition of the reagents. CaO was heated at 1200 °C for 12 hours to remove any type of water before using as initial slag former. The four constituents were weighed carefully in the required proportions and mixed thoroughly in a mixing mill. Mixtures were heated to 1000 °C at 10 °C/min heating rate and held for half an hour to decompose Na_2CO_3. After decomposition and dehydration the mixture was finely ground and pressed to pellets.

2.2 Experiment procedure

A pellet of the pre-melted slag mixture (~5g) was placed in a platinum crucible and positioned into a box furnace for melting. After fusion, each sample was cooled down to room temperature and finely ground. This process was repeated two or three times to ensure the homogeneity of the slag samples, according to the appearance on the samples. Subsequently, differential scanning calorimetry (DSC) was employed to determine the melting temperature. The sample (~10mg) was charged into a platinum crucible, and heated up by the rate of 10 °C/min under argon atmosphere with a flow rate of 30 ml/min.

For the equilibrium experiments, each ground sample was wrapped in a platinum foil and placed in an electrical resistance tube furnace. The temperature of the furnace was measured with a Pt-PtRh10 thermocouple which was calibrated against a standard thermocouple and the temperature accuracy was estimated to be within ±2 °C. The samples were first re-ground and re-melted for several times when it is necessary to ensure the formation of a homogeneous melt. The samples were subsequently equilibrated at a temperature 10 °C to 20 °C lower than the melting temperature determined by DSC experiments. Careful consideration was given to the equilibration time, which was different depending on the sample composition and temperature. Repeating experiments with longer equilibration time were performed for a number of samples to check whether the real equilibrium was achieved. After the equilibrium, the sample was rapidly taken out from the furnace and quenched to room temperature under high pressure nitrogen atmosphere.

The quenched samples were embedded in epoxy resin and subsequently polished for microscopic analysis. A JEOL electron probe X-ray microanalyzer (EPMA) (JXA-8800, JEOL, Japan) was used for microstructural and compositional analysis of the phases in the samples. X-ray diffraction (XRD) (Model D5005, Bruker, Germany) analysis was used to confirm the phases identified with the EPMA analysis.

2.3 Experimental design

High temperature equilibrium relationships of the systems $CaO{\cdot}SiO_2$─$Na_2O{\cdot}Al_2O_3{\cdot}6SiO_2$ and $CaO{\cdot}SiO_2$─$Na_2O{\cdot}Al_2O_3{\cdot}2SiO_2$─$Na_2O{\cdot}Al_2O_3{\cdot}6SiO_2$ were reported by Foster [12]. Moir and Glasser [13] studied the phase equilibria in the glass-forming region of the system CaO─Al_2O_3─SiO_2─Na_2O. Based on these literature, the reaction region of the primary phases in the system $CaO{\cdot}SiO_2$─$Na_2O{\cdot}SiO_2$─$Na_2O{\cdot}Al_2O_3{\cdot}6SiO_2$ will be located in the composition range of 40 wt % ~ 80 wt% $Na_2O{\cdot}Al_2O_3{\cdot}6SiO_2$. Therefore, approximately 40 samples were prepared in this region, and the compositions as well as equilibrium temperatures are given in Table 1. The experiments were carried out in the temperature range from 800 °C to 1200 °C. The liquidus surface and phase relations of the primary phase fields were investigated according to the experimental results.

Because of the high volatility of Na_2O, the preparation of the slag mixtures was done very carefully. Preliminary heating at 850 °C was conducted firstly before the samples were raised to their fusion temperatures. This precaution can prevent considerable volatilization of Na_2O. After heating at this temperature, the samples were weighed to determine the weight loss. Then the mixtures were heated at higher temperatures than their melting temperature. After cooling to room temperature, the samples were weighed again and ground. This step was repeated twice or three times. For the sample with significant weight loss, additional Na_2CO_3 was added. The composition of some quenched samples was analyzed with X-ray fluorescence (XRF) (Model PW 2400, Philips, The Netherlands) for the final equilibrium composition determination. According to the weighing and analyzing results, the volatilization losses of samples did not have much effect on the bulk composition. They were in the controlling error margin, which was also attributed by the fact that all the samples in the present work contain relatively low Na_2O and all the fusion temperatures are lower than 1200 °C.

Table 1. Experimental conditions and results of the system $CaO{\cdot}SiO_2$–$Na_2O{\cdot}SiO_2$–$Na_2O{\cdot}Al_2O_3{\cdot}6SiO_2$

Sample	Compositions (wt %)			Time (h)	Liquidus temperature (± 2 °C)	Equilibrium temperature (± 2 °C)	Phases in equilibrium
	$CaO{\cdot}SiO_2$	$Na_2O{\cdot}SiO_2$	$Na_2O{\cdot}Al_2O_3{\cdot}6SiO_2$				
Primary phase $CaSiO_3$							
1	25.0	5.0	70.0	8	1080	1100	L
2	28.4	5.6	66.0	8	1100	1070	L+CS
3	32.5	6.5	61.0	6	1120	1100	L+CS
4	35.0	7.0	58.0	7	1135	1150	L
				6		1100	L+CS
5	37.0	9.0	54.0	9	1150	1150	L+CS
Primary phase $NaAlSi_3O_8$							
6	22.7	11.3	66.0	18	1053	1030	L+Plagioclase
7	26.0	13.0	61.0	24	1035	1020	L+Plagioclase
8	12.5	12.5	75.0	18	1188	1160	L+Plagioclase
9	15.0	15.0	70.0	20	1153	1140	L+Plagioclase
10	17.0	17.0	66.0	18	1050	1060	L
				15		1020	L+Plagioclase
11	19.5	19.5	61.0	15	1010	1000	L+Plagioclase
12	8.3	16.7	75.0	20	1176	1160	L+Plagioclase
13	10.0	20.0	70.0	18	1151	1135	L+Plagioclase
14	11.3	23.7	66.0	12	1042	1045	L
				10		1030	L+Plagioclase
15	13.0	26.0	61.0	14	980	960	L+Plagioclase
16	8.0	26.0	66.0	14	1020	1000	L+Plagioclase
17	9.0	30.0	61.0	14	960	960	L
				14		940	L+Plagioclase
18	4.0	30.0	66.0	14	1000	980	L+Plagioclase
19	5.0	34.0	61.0	16	941	930	L+Plagioclase
20	2.0	32.0.0	66.0	12	984	950	L+Plagioclase
21	3.0	36.0	61.0	15	900	880	L+Plagioclase
Primary phase NC_2S_3							
22	28.0	14.0	58.0	8	1036	1050	L
				8		1020	L+ NC_2S_3
23	30.7	15.3	54.0	6	1056	1060	L
				8		1030	L+ NC_2S_3
24	33.3	16.7	50.0	4	1082	1100	L
25	21.0	21.0	58.0	8	1030	1000	L+ NC_2S_3
26	23.0	23.0	54.0	5	1044	1050	L
				5		1020	L+ NC_2S_3
27	25.0	25.0	50.0	6	1063	1050	L+ NC_2S_3
28	27.5	27.5	45.0	8	1078	1100	L
29	14.0	28.0	58.0	8	961	940	L+ NC_2S_3
30	15.3	31.7	54.0	10	1000	980	L+ NC_2S_3
				12		960	L+ NC_2S_3+ N_2CS_3
31	36.7	18.3	45.0	8	1066	1050	L+ NC_2S_3
Primary phase N_2CS_3							
32	10.0	32.0	58.0	8	928	920	L+ N_2CS_3
33	38.0	12.0	50.0	10	1017	1000	L+ N_2CS_3
34	6.0	36.0	58.0	10	908	900	L+ N_2CS_3
35	6.0	40.0	54.0	10	942	930	L+ N_2CS_3
36	7.0	43.0	50.0	10	1090	1000	L
Primary phase NS							
37	3.0	39.0	58.0	8	900	880	L+ NS
38	3.0	43.0	54.0	6	950	940	L+ NS
39	3.0	47.0	50.0	8	1005	980	L+ NS

L= Liquid; C=CaO; N=Na_2O; S=SiO_2; NS=$Na_2O{\cdot}SiO_2$; CS=$CaO{\cdot}SiO_2$=NC_2S_3=$Na_2O{\cdot}2CaO{\cdot}3SiO_2$; N_2CS_3=$2Na_2O{\cdot}CaO{\cdot}3SiO_2$; Plagioclase=$Na_2O{\cdot}Al_2O_3{\cdot}6SiO_2$ (Albite s.s.).

3. Results and discussion

3.1 Thermal behavior and liquidus temperature

Due to the pretreatment as mentioned in the experimental procedure, the samples used for the DSC measurements were homogeneous in terms of composition. When samples were heated with 10 °C/min during the DSC test, melting reactions take place shown as endothermic peaks in Figure 2. The first shift from the baseline in the DSC curve can be considered as a good estimate of the solidus temperature. Moreover, the DSC melting peak range is broad for the present investigated samples, and the onset and endpoint temperatures determined by the tangent method are different from the first shift. On the other hand, the endpoint temperature of the peak suffers from the heating rate, which may lead to a higher value than the real liquidus temperature. Therefore, the onset temperature (taken in the intersection of straight lines tangent to the base line and the low-temperature side of the peak) is taken as the liquidus temperature (T_m) of the corresponding endothermic peaks. Figure 2 shows the DSC test results of three typical samples, numbered with 11, 16 and 25 bear-by the 1000 °C isotherm as shown in Figure 3. The melting temperatures of these three samples are 1010 °C, 1020 °C and 1030 °C, respectively.

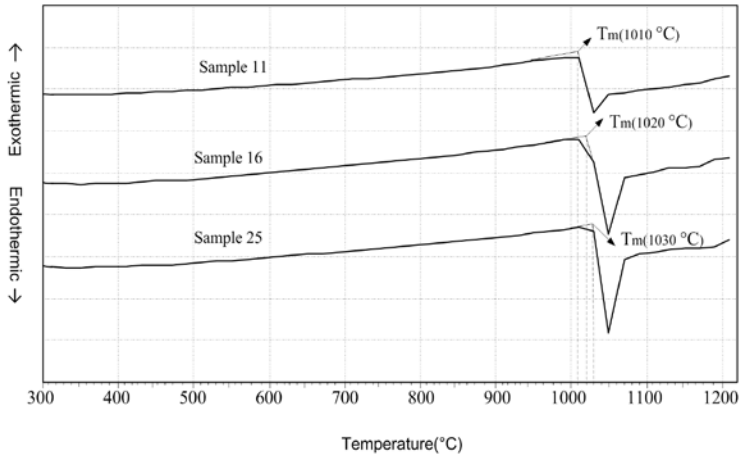

Fig. 2 DSC curves of samples 11, 16 and 25
(The liquidus temperature T_m and sample compositions are given in Table 1)

The liquidus temperatures and equilibration results of all samples are given in Table 1. The liquidus surface projection in the 40 wt% ~ 80 wt% $Na_2O{\cdot}Al_2O_3{\cdot}6SiO_2$ region of the system $CaO{\cdot}SiO_2$─-$Na_2O{\cdot}SiO_2$─-$Na_2O{\cdot}Al_2O_3{\cdot}6SiO_2$ were constructed by manually fitting the experimental data to a surface as shown in Figure 3, which simultaneously shows the portion of the system containing the primary $CaO{\cdot}SiO_2$, $Na_2O{\cdot}SiO_2$, $Na_2O{\cdot}2CaO{\cdot}3SiO_2$, $2Na_2O{\cdot}CaO{\cdot}3SiO_2$ and $Na_2O{\cdot}Al_2O_3{\cdot}6SiO_2$ phase fields and three invariant points.

3.2 Phase relations

In Foster's [12] work, the phase relations of the binary $CaO{\cdot}SiO_2$─$Na_2O{\cdot}Al_2O_3{\cdot}6SiO_2$ were investigated and the $CaO{\cdot}SiO_2$ phase field was established. The liquidus temperatures of the above binary system from Foster [12] were employed in the present work. For the $CaO{\cdot}SiO_2$ primary phase field, five compositional points were selected to investigate the boundary and liquidus temperature using EPMA and XRD measurements. The region close to the $CaO{\cdot}SiO_2$ corner, in which the liquidus temperatures are very high, was not investigated in the present work. The phase field of $CaO{\cdot}SiO_2$ is bounded by the primary phase fields of $Na_2O{\cdot}2CaO{\cdot}3SiO_2$ and $Na_2O{\cdot}Al_2O_3{\cdot}6SiO_2$ as shown in Figure 3. Sample 3 in the $CaO{\cdot}SiO_2$ phase field was equilibrated at 1100 °C. The compound $CaO{\cdot}SiO_2$ was identified

needle-shaped in the backscattered electron image. The EPMA and XRD results of it shown in Figure 4 indicate that the phase $CaO{\cdot}SiO_2$ is in equilibrium with liquid at the composition of 32.5 wt% $CaO{\cdot}SiO_2$, 6.5 wt% $Na_2O{\cdot}SiO_2$ and 61.0 wt% $Na_2O{\cdot}Al_2O_3{\cdot}6SiO_2$.

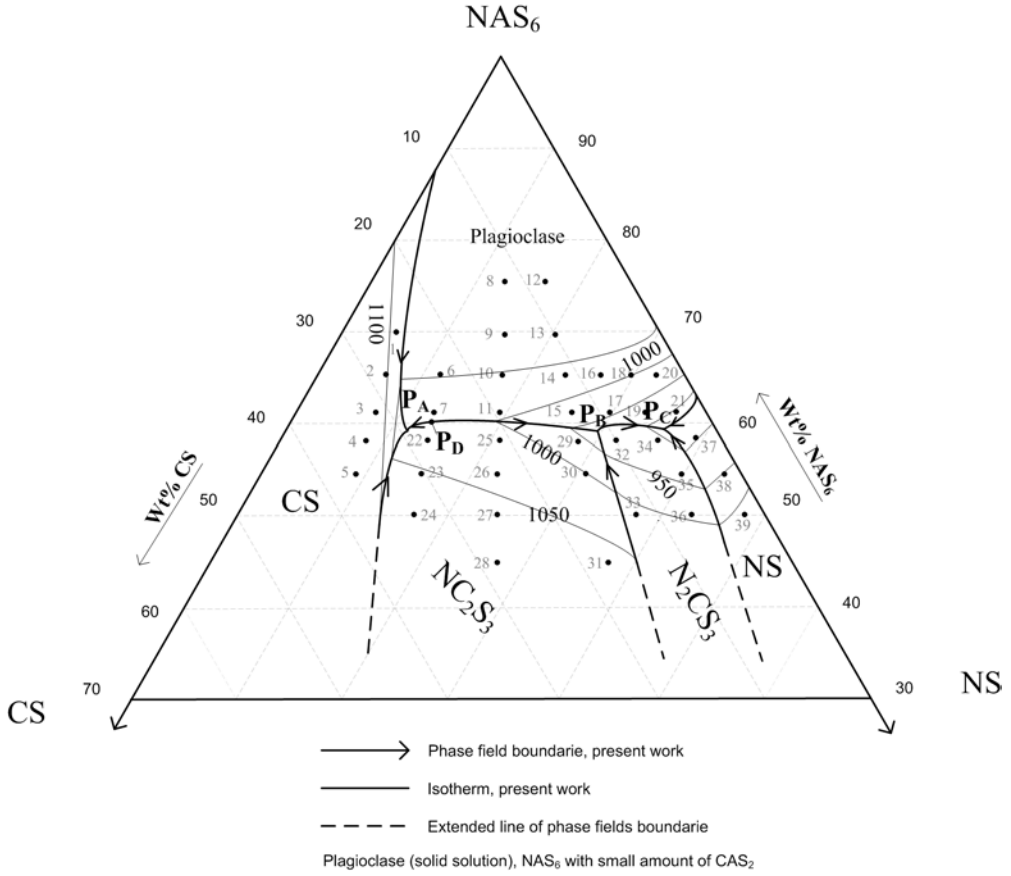

Fig. 3 The equilibrium diagram for the system $CaO{\cdot}SiO_2$─$Na_2O{\cdot}SiO_2$─$Na_2O{\cdot}Al_2O_3{\cdot}6SiO_2$ containing $Na_2O{\cdot}Al_2O_3{\cdot}6SiO_2$ (30-70 wt%). Invariant points (compositions and temperatures are given in Table 2) are labeled as P_A, P_B and P_C. P_D is the highest temperature point (at 26 wt% $CaO{\cdot}SiO_2$, 14 wt% $Na_2O{\cdot}SiO_2$ and 60 wt% $Na_2O{\cdot}Al_2O_3{\cdot}6SiO_2$ and 1035 °C) on the boundary curve P_AP_B. The samples are labeled as Arabic numerals according to Table 1 (A=Al_2O_3; C=CaO; N=Na_2O; S=SiO_2).

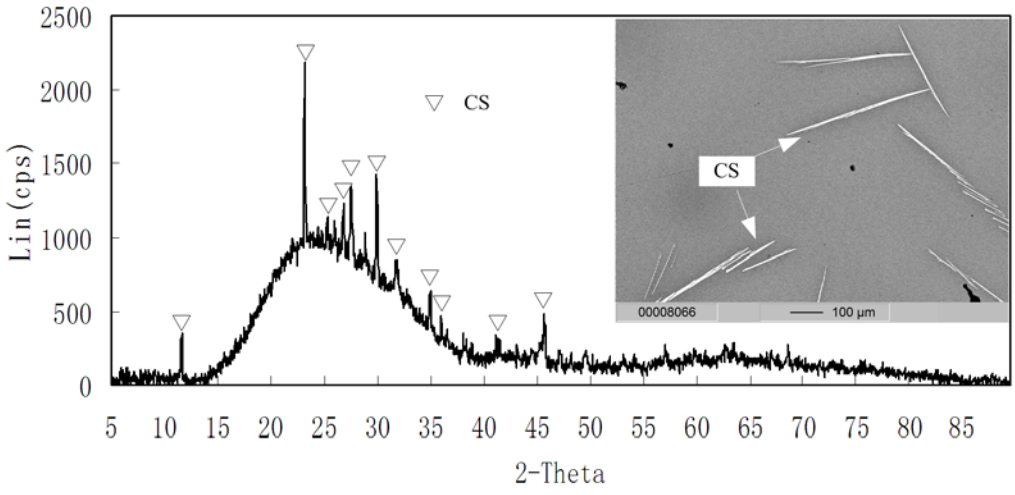

Fig. 4 Backscattered electron image and X-ray diffraction patterns of sample 3 quenched at 1100 °C (C=CaO; S=SiO_2).

In the present work a portion of the $Na_2O{\cdot}2CaO{\cdot}3SiO_2$ phase field was investigated by EPMA and XRD measurements. The $Na_2O{\cdot}2CaO{\cdot}3SiO_2$ phase field is bordered by $CaO{\cdot}SiO_2$, $2Na_2O{\cdot}CaO{\cdot}3SiO_2$ and $Na_2O{\cdot}Al_2O_3{\cdot}6SiO_2$ in the 40 wt% ~ 80 wt% $Na_2O{\cdot}Al_2O_3{\cdot}6SiO_2$ region. The liquidus temperature in $Na_2O{\cdot}2CaO{\cdot}3SiO_2$ phase field determined in the present work is from 950 °C to 1100 °C. The sample 30 shown in Table 1 with 15.3 wt% $CaO{\cdot}SiO_2$, 31.7 wt% $Na_2O{\cdot}SiO_2$ and 54.0 wt% $Na_2O{\cdot}Al_2O_3{\cdot}6SiO_2$ was equilibrated at 980 °C and 960 °C. Crystal phase $Na_2O{\cdot}2CaO{\cdot}3SiO_2$ in equilibrium with amorphous glass can be identified when the sample was quenched at 980 °C. The backscattered electron image and XRD result shown in Figure 5 indicate that phase $Na_2O{\cdot}2CaO{\cdot}3SiO_2$ coexists with $2Na_2O{\cdot}CaO{\cdot}3SiO_2$ and glass when the sample was quenched at 960 °C. When the equilibrium temperature of sample 30 is decreasing, the reaction will go along with the boundary curve that lies between the $Na_2O{\cdot}2CaO{\cdot}3SiO_2$ and $2Na_2O{\cdot}CaO{\cdot}3SiO_2$ phase fields as shown in Figure 3. Therefore, these two phases can be found simultaneously. From the primary phase field of $Na_2O{\cdot}2CaO{\cdot}3SiO_2$, shown in Figure 3, it can be seen that this phase is compatible with $CaO{\cdot}SiO_2$, $2Na_2O{\cdot}CaO{\cdot}3SiO_2$ and $Na_2O{\cdot}Al_2O_3{\cdot}6SiO_2$ in the presence of liquid.

The incongruently melting phase $2Na_2O{\cdot}CaO{\cdot}3SiO_2$ indicated by Shahid and Glasser [14] in their investigation was also observed by EPMA and XRD measurements in this study. The primary phase field of this compound was studied in the temperature range 900 °C ~ 1050 °C in the present work. It is bordered by $Na_2O{\cdot}SiO_2$, $Na_2O{\cdot}2CaO{\cdot}3SiO_2$ and $Na_2O{\cdot}Al_2O_3{\cdot}6SiO_2$ phase fields as shown in Figure 3. Samples 32 and 34 containing the same amount of $Na_2O{\cdot}Al_2O_3{\cdot}6SiO_2$ (58.0 wt%) were quenched from 920 °C and 900 °C, respectively. The results indicated that phase $2Na_2O{\cdot}CaO{\cdot}3SiO_2$ coexists with liquid at these two different temperatures. Three samples were examined in the $Na_2O{\cdot}SiO_2$ phase field and the isotherms of this phase field were established as shown in Figure 3.

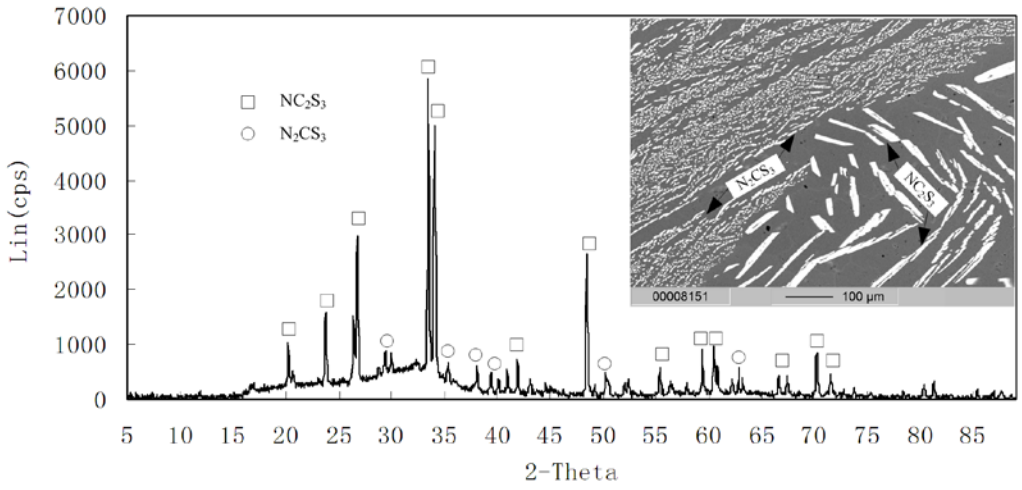

Fig. 5 Backscattered electron image and X-ray diffraction patterns of sample 30 quenched at 960 °C (N=Na_2O; C=CaO; S=SiO_2).

Characteristics of the phase $Na_2O{\cdot}Al_2O_3{\cdot}6SiO_2$ was reported by Foster [12] in 1942. The experimental results in his work indicated that the crystals were not a pure $Na_2O{\cdot}Al_2O_3{\cdot}6SiO_2$ compound (= albite s.s.) but rather a plagioclase bearing a small amount of $CaO{\cdot}Al_2O_3{\cdot}2SiO_2$ in solid solution. This was also confirmed by the work of Moir and Glasser [13]. In the present study, the plagioclase field was investigated in the composition region of less than 75.0 wt%

$Na_2O{\cdot}Al_2O_3{\cdot}6SiO_2$. The equilibrium temperatures covered from 850 °C to 1200 °C. The plagioclase ($NaAlSi_3O_8$ solid solution) field is bordered by $Na_2O{\cdot}SiO_2$, $CaO{\cdot}SiO_2$, $Na_2O{\cdot}2CaO{\cdot}3SiO_2$ and $2Na_2O{\cdot}CaO{\cdot}3SiO_2$ phase fields. Sample 14 shown in Table 1 with 11.3 wt% $CaO{\cdot}SiO_2$, 12.7 wt% $Na_2O{\cdot}SiO_2$ and 66.0 wt% $Na_2O{\cdot}Al_2O_3{\cdot}6SiO_2$ was equilibrated at 1045 °C and 1030 °C. Due to the melting temperature of this sample, determined to be 1042 °C in this study by DSC measurement, no feldspar crystals were obtained when the sample was quenched at 1045 °C. The EPMA and XRD measurement results of this sample quenched at 1030 °C are given in Figure 6. The plagioclase was identified in the backscattered electron image and XRD analysis. It is in agreement with Foster's work [12]. Because $CaO{\cdot}Al_2O_3{\cdot}2SiO_2$ is only in a small amount in the solid solution, the phase $Na_2O{\cdot}Al_2O_3{\cdot}6SiO_2$ is the primary wave crest in the XRD pattern. The backscattered electron image of this equilibration test shows that the plagioclase coexists with liquid at 1030 °C.

Five phase fields $Na_2O{\cdot}SiO_2$, $CaO{\cdot}SiO_2$, $Na_2O{\cdot}2CaO{\cdot}3SiO_2$, $2Na_2O{\cdot}CaO{\cdot}3SiO_2$ and $Na_2O{\cdot}Al_2O_3{\cdot}6SiO_2$ were established by the equilibrium experiments shown in Table 1. The isotherms as shown in Figure 3 in the interesting area of the $CaO{\cdot}SiO_2$–$Na_2O{\cdot}SiO_2$–$Na_2O{\cdot}Al_2O_3{\cdot}6SiO_2$ system was studied through the DSC measurements. Therefore, the boundary curves between the phase fields and the temperature tendency on the curves can be deduced. Because of congruently melting of the compound $Na_2O{\cdot}2CaO{\cdot}3SiO_2$, it can be concluded that there is a highest temperature point P_D on the boundary curve AB between $Na_2O{\cdot}2CaO{\cdot}3SiO_2$ and $Na_2O{\cdot}Al_2O_3{\cdot}6SiO_2$ phase fields as shown in Figure 3.

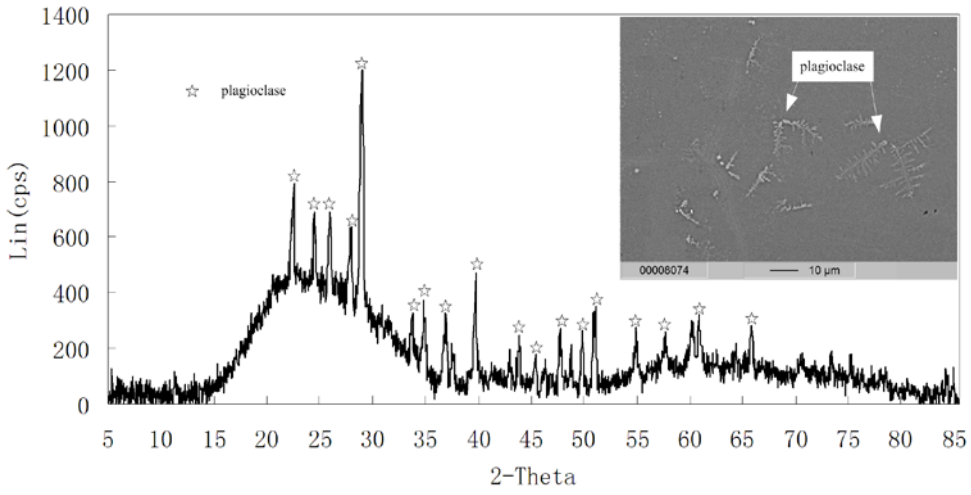

Fig. 6 Backscattered electron image and X-ray diffraction patterns of sample 14 quenched at 1030 °C, plagioclase (solid solution, $Na_2O{\cdot}Al_2O_3{\cdot}6SiO_2$ with small amount of $CaO{\cdot}Al_2O_3{\cdot}2SiO_2$).

Sample 3, 7 and 22 as shown in Table 1 were equilibrated at 1100 °C, 1020 °C and 1020 °C, respectively. Three different phases $CaO{\cdot}SiO_2$, $Na_2O{\cdot}2CaO{\cdot}3SiO_2$ and $Na_2O{\cdot}Al_2O_3{\cdot}6SiO_2$ were identified in these samples. Fitting all these temperature and equilibrium data into the liquidus surface, it can be concluded that $Na_2O{\cdot}Al_2O_3{\cdot}6SiO_2$ is in equilibrium with $CaO{\cdot}SiO_2$ and $Na_2O{\cdot}2CaO{\cdot}3SiO_2$ at the eutectic point P_A, having the composition of 29.0 wt% $CaO{\cdot}SiO_2$, 12.0 wt% $Na_2O{\cdot}SiO_2$ and 59.0 wt% $Na_2O{\cdot}Al_2O_3{\cdot}6SiO_2$ at temperature of 1030 °C, as shown in Figure 3 and Table 2. Temperature decreases from the highest temperature point P_D to point P_B following the arrow on the boundary P_AP_B. Phases $Na_2O{\cdot}2CaO{\cdot}3SiO_2$ and $Na_2O{\cdot}Al_2O_3{\cdot}6SiO_2$ coexisting with liquid were observed in sample 29

and 17 at 940 °C as shown in Table 1, respectively. The incongruently melting phase $2Na_2O{\cdot}CaO{\cdot}3SiO_2$ was identified in sample 32 at equilibrating temperature of 920 °C. Therefore, for phases $Na_2O{\cdot}2CaO{\cdot}3SiO_2$, $2Na_2O{\cdot}CaO{\cdot}3SiO_2$ and $Na_2O{\cdot}Al_2O_3{\cdot}6SiO_2$, the point P_B can be established as a peritectic point with composition of 13.0 wt% $CaO{\cdot}SiO_2$, 29.0 wt% $Na_2O{\cdot}SiO_2$ and 58.0 wt% $Na_2O{\cdot}Al_2O_3{\cdot}6SiO_2$ at 930 °C. Based on the equilibrium experiments, another eutectic point P_C among phases of $2Na_2O{\cdot}CaO{\cdot}3SiO_2$, $Na_2O{\cdot}SiO_2$ and $Na_2O{\cdot}Al_2O_3{\cdot}6SiO_2$ was simultaneously determined at 5.0 wt% $CaO{\cdot}SiO_2$, 35.0 wt% $Na_2O{\cdot}SiO_2$ and 60.0 wt% $Na_2O{\cdot}Al_2O_3{\cdot}6SiO_2$ at 880 °C. The compositions and temperatures of these three ternary invariant points in the system $CaO{\cdot}SiO_2$─$Na_2O{\cdot}SiO_2$─$Na_2O{\cdot}Al_2O_3{\cdot}6SiO_2$ are given in Table 2.

Table 2. The compositions and temperatures of ternary invariant points in the system $CaO{\cdot}SiO_2$─$Na_2O{\cdot}SiO_2$─$Na_2O{\cdot}Al_2O_3{\cdot}6SiO_2$

Invariant point	Phases	Reaction Type	Composition (wt %)			Temperature (°C)
			CS	NS	NAS_6	
P_A	NAS_6-CS- NC_2S_3	Eutectic	29	12	59	1030
P_B	NAS_6- NC_2S_3-N_2CS_3	Peritectic	13	29	58	930
P_C	NAS_6- N_2CS_3-NS	Eutectic	5	35	60	880

NS=$Na_2O{\cdot}SiO_2$; CS=$CaO{\cdot}SiO_2$; NC_2S_3=$Na_2O{\cdot}2CaO{\cdot}3SiO_2$; N_2CS_3=$2Na_2O{\cdot}CaO{\cdot}3SiO_2$; NAS_6=$Na_2O{\cdot}Al_2O_3{\cdot}6SiO_2$

4. Conclusions

Phase relations in the composition range of 40 wt% ~ 80 wt% $Na_2O{\cdot}Al_2O_3{\cdot}6SiO_2$ of the system $CaO{\cdot}SiO_2$─$Na_2O{\cdot}SiO_2$─$Na_2O{\cdot}Al_2O_3{\cdot}6SiO_2$, which are important for bottom ash application, were newly established in the present work. Five primary phase fields, $CaO{\cdot}SiO_2$, $Na_2O{\cdot}SiO_2$, $Na_2O{\cdot}2CaO{\cdot}3SiO_2$, $2Na_2O{\cdot}CaO{\cdot}3SiO_2$ and $Na_2O{\cdot}Al_2O_3{\cdot}6SiO_2$ in this system have been investigated in the temperature range from 800 °C to 1200 °C. The liquidus temperatures and invariant points of the phase fields, which were not found in literature, were determined. Eutectic point P_A with the composition of 29.0 wt% $CaO{\cdot}SiO_2$, 12.0 wt% $Na_2O{\cdot}SiO_2$ and 59.0 wt% $Na_2O{\cdot}Al_2O_3{\cdot}6SiO_2$ at temperature 1030 °C was established among $CaO{\cdot}SiO_2$, $Na_2O{\cdot}2CaO{\cdot}3SiO_2$ and $Na_2O{\cdot}Al_2O_3{\cdot}6SiO_2$ phase fields. Peritectic reaction of phase $Na_2O{\cdot}2CaO{\cdot}3SiO_2$, $2Na_2O{\cdot}CaO{\cdot}3SiO_2$ and $Na_2O{\cdot}Al_2O_3{\cdot}6SiO_2$ takes place at 930 °C. The temperature of the ternary eutectic point P_C was verified at 880 °C with composition 5.0 wt% $CaO{\cdot}SiO_2$, 35.0 wt% $Na_2O{\cdot}SiO_2$ and 60.0 wt% $Na_2O{\cdot}Al_2O_3{\cdot}6SiO_2$.

Acknowledgement

This work was supported by the Royal Netherlands Academy of Arts and Science (KNAW) under project 10CDP026 and by the National Natural Science Foundation of China Grant No.50974034. XRD analyses from the analytical group in the Department of Materials Science and Engineering, Delft University of Technology, are acknowledged.

References

[1] C. R. Cheeseman, S. Monteiro da Rocha, C. Sollars, S. Bethanis, A. R. Boccaccini, Ceramic processing of incinerator bottom ash. Waste Management, 2003, 23, p907-916.

[2] E. J. Dykstra, T. T.Eighmy. Petrogenesis of municipal solid waste combustion bottom ash. Applied Geochemistry, 1998, 14(1999), p1073-1091.

[3] Y. Xiao, M. Oorsprong, Y. Yang, J. Voncken. Vitrification of Bottom Ash from a Municipal Solid Waste Incinerator. Waste Management, 2008, 28, p1020-1206.

[4] L. Barbieri, A. C. Lancellotti. Alkaline and Alkaline-earth Silicate Glasses and Glass-ceramics from Municipal and Industrial Wastes. Journal of the European Ceramic Society, 2000, 20, p2477-83.

[5] M. Ferraris, M. Salvo. Glass Matrix Composites from Solid Waste Materials. Journal of the European Ceramic Society, 2001, 21, p453-60.

[6] M. Li, J. Xiang. Characterization of Solid Residues from Municipal Solid Waste Incinerator. Fuel, 2004, 83, p1397-405.

[7] G. W. Morey, N. L. Bowen. Ternary System Sodium Metasilicate-Calcium Metasilicate –Silica. Journal of the Glass Technology Society, 1925, 9 (35), p226-64.

[8] G. W. Morey. The Devitrification of Soda-Lime-Silica Glasses. Journal of the American Ceramic Society, 1930, 13, p683-713.

[9] Z. Zhang, Y. Xiao, J. Voncken, Y. Yang, R. Boom, N. Wang, Z, Zong. Phase Equilibria in the Na_2O-CaO-SiO_2 System. Journal of the American Ceramic Society, 2011, 94(9), p3088-3093.

[10] J, Spivak. The System $NaAlSiO_4$─$CaSiO_3$─Na_2SiO_3. The Journal of Geology, 1944, 52, p24-52.

[11] W. K. Gummer. The System $CaSiO_3$─ $CaAl_2Si_2O_8$─$NaAlSiO_4$. The Journal of Geology, 1943, 21, p503-530.

[12] W. R. Foster. The System $NaAlSi_3O_8$-$CaSiO_3$-$NaAlSiO_4$. The Journal of Geology, 1942, 50, p152-173.

[13] G. K. Moir, F. P. Glasser. Physics and Chemistry of Glasses, 1976, 17(3), p45-53.

[14] K.A. Shahid, F. P. Glasser. Phase Equilibria in the Glass Forming Region of the System Na_2O─CaO─SiO_2. Physics and Chemistry of Glasses, 1971, 12(2), p50-57.